D-Cycloserine Ameliorates Autism-Like Deficits by Removing GluA2-Containing AMPA Receptors in a Valproic Acid-Induced Rat Model

Han-Fang Wu, Po See Chen, Ya-Ting Hsu, Chi-Wei Lee, Tzu-Feng Wang, Yi-Ju Chen & Hui-Ching Lin

Molecular Neurobiology

ISSN 0893-7648

Mol Neurobiol
DOI 10.1007/s12035-017-0685-1

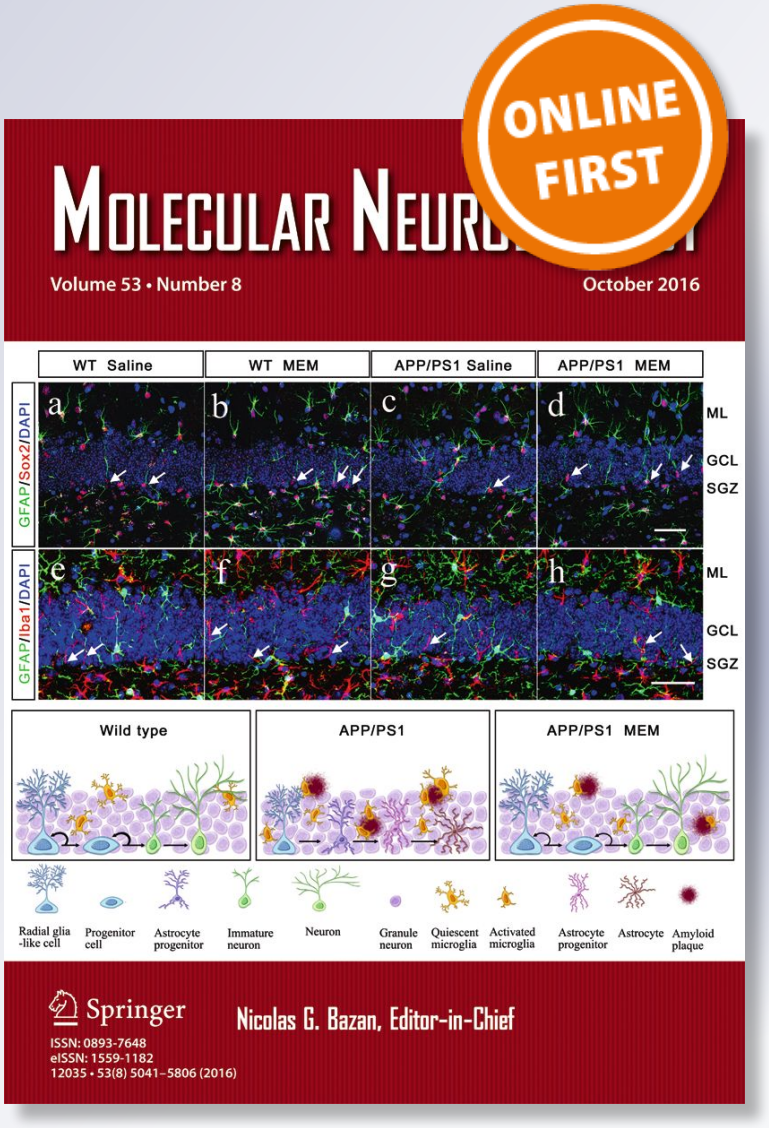

Springer

Mol Neurobiol
DOI 10.1007/s12035-017-0685-1

D-Cycloserine Ameliorates Autism-Like Deficits by Removing GluA2-Containing AMPA Receptors in a Valproic Acid-Induced Rat Model

Han-Fang Wu[1] · Po See Chen[2,3] · Ya-Ting Hsu[1] · Chi-Wei Lee[1] · Tzu-Feng Wang[2,4] · Yi-Ju Chen[1] · Hui-Ching Lin[1,5,6]

Received: 19 April 2017 / Accepted: 10 July 2017

Abstract Valproic acid (VPA)-exposed rat offspring have demonstrated autism spectrum disorder (ASD) phenotypes and impaired N-methyl-D-aspartate receptor (NMDAR)-dependent long-term depression (LTD) in the lateral nucleus of the amygdala. NMDAR partial agonist D-cycloserine (DCS) has been reported to act as a cognitive enhancer by increasing the NMDAR response to improve autistic-like phenotypes in animals. However, the mechanism of DCS in alleviating the ASD is still unknown. Using combined behavioral, electrophysiological, and molecular approaches, we found that DCS administration rescued social interaction deficits and anxiety/repetitive-like behaviors observed in VPA-exposed offspring. In the amygdala synapses, DCS treatment reversed the decreased paired pulse ratio (PPR) and the impaired NMDAR-dependent LTD, increased the frequency and amplitude of miniature excitatory postsynaptic currents (mEPSCs), and resulted in a higher dendritic spine density at the amygdala synapses in the VPA-exposed offspring. Moreover, we found that DCS facilitated the removal of GluA2-containing α-amino-3-hydroxy-5-methyl-4-isoxazolepropionic acid receptors (GluA2/AMPARs) by inducing NMDAR-dependent LTD in the VPA-exposed offspring. We further established that the effects of DCS treatment, including increased GluA2/AMPAR removal and rescues of impaired social behavior, were blocked by Tat-GluA2$_{3Y}$, a GluA2-derived peptide that disrupted regulation of AMPAR endocytosis. These results provided the first evidence that rescue of the ASD-like phenotype by DCS is mediated by the mechanism of GluA2/AMPAR removal in VPA-exposed rat offspring.

Keywords Autism spectrum disorder · D-Cycloserine · Long-term depression · NMDARs · GluA2/AMPARs · Valproic acid

✉ Hui-Ching Lin
hclin7@ym.edu.tw; huiching4372@gmail.com

[1] Department and Institute of Physiology, School of Medicine, National Yang-Ming University, Taipei 11221, Taiwan

[2] Department of Psychiatry, National Cheng Kung University Hospital, College of Medicine, National Cheng Kung University, Tainan 70101, Taiwan

[3] Addiction Research Center, National Cheng Kung University, Tainan 70101, Taiwan

[4] Taiwan International Graduate Program in Interdisciplinary Neuroscience, National Cheng Kung University and Academia Sinica, Taipei, Taiwan

[5] Brain Research Center, National Yang-Ming University, Taipei 11221, Taiwan

[6] Ph.D. Program for Neural Regenerative Medicine, College of Medical Science and Technology, Taipei Medical University, Taipei 11031, Taiwan

Introduction

Autism spectrum disorder (ASD), a neurodevelopmental disorder, is characterized by impaired social interaction, communication deficits, and restricted and repetitive interests/behaviors [1–4]. There is commonly for four times more prevalent in males compared to female in ASD [5, 6]. The mechanisms that underlie the cognitive deficits associated with ASD result from imbalances in synaptic excitation and inhibition neurotransmission, leading to abnormal synaptic flexibility [7]. The

Published online: 21 July 2017

glutamatergic systems are involved in regulating the molecular and cellular mechanisms of synaptic plasticity in ASD. More recently, N-methyl-D-aspartate receptor (NMDAR) dysfunction has also been thought to contribute to ASD. *Shank2*$^{-/-}$ mice have been reported to exhibit reduced hippocampal NMDAR function and sociability [8]. In addition, *IRSp53*$^{-/-}$ mice exhibit an increased NMDA/α-amino-3-hydroxy-5-methyl-4-isoxazolepropionic acid (AMPA) receptor ratio and greater social deficits suggesting a change in NMDAR function, resulting in ASD-like patterns [9].

$_{D}$-Cycloserine ($_{D}$-4-amino-3-isoxazolidone; DCS) is a partial agonist at the glycine binding site on the NMDA subtype of excitatory receptor. Modulation of NMDARs by a partial agonist is more useful for research than a direct agonist of the glutamate receptor, which produces the side effects including seizures and neurotoxicity [10]. DCS has been shown to act as a potential cognitive enhancer for the treatment of anxiety disorder, phobias, obsessive-compulsive behavior, and schizophrenia [11–13]. A previous study reported that DCS facilitated the acquisition and retrieval of fear extinction memory by enhancing the expression of NMDAR subunit NR2B [14]. DCS is also known to ameliorate social abnormality and repetitive behavior significantly in individuals with ASD [15–18]. In NMDAR dysfunction animal models of ASD, including *Neuroligin1*$^{-/-}$ and *Shank2*$^{-/-}$ mice, repetitive behavior and impaired sociability are observed, which are rescued by DCS treatment [8, 19].

Ramanathan et al. observed that the deletion of chromosomal region contains AMPAR gene that encodes GluA2/AMPARs in autistic patient [20]. Deletion of Gria2 genes encoding AMPAR subunits reduced anxious-like behavior [21]. Interestingly, a recent study found that knockdown of Gria2 also alleviated the social deficits in frontotemporal dementia animal model suggesting the GluA2/AMPA involved in regulating the cognitive function [22]. The alteration of synaptic plasticity resulting from aberrant AMPAR internalization may contribute to cognitive deficit in the fragile X syndrome (FXS) autism model [23]. By binding to the glycine site on the NMDAR NR1 subunit, DCS facilitates low-frequency stimulation (LFS)-induced depotentiation and NMDAR-dependent long-term depression (NMDAR-LTD) in the amygdala and hippocampus, respectively [14, 24]. In addition, DCS improves fear extinction by increasing GluA1- and GluA2-containing AMPAR (GluA1/AMPAR and GluA2/AMPAR) endocytosis [25]. These results indicated the possibility that DCS may modulate AMPARs and further alter the synaptic plasticity in ASD. The results of our recent study showed that rodent exposure to valproic acid (VPA) in utero led to dysfunction of NMDARs, and further impaired NMDAR-LTD in the amygdala [26].

In the current study, we examined whether DCS reversed autistic-like behaviors and affected the synaptic plasticity of LTD in the VPA-exposed offspring. We further examined whether the DCS modulated the GluA2/AMPARs, which play an important role in activity-dependent internalization and are involved in regulating social behaviors and NMDAR-LTD in the VPA-induced ASD model. We demonstrated that DCS normalized autism-like behaviors via the mechanism of GluA2/AMPAR endocytosis in the lateral amygdala synapses of the VPA-exposed offspring by acting on NMDARs.

Material and Methods

Animals

All procedures were approved by the Experimental Animal Review Committee at National Yang-Ming University. Sprague Dawley (SD) rats were housed 4~5 to a cage in a temperature-controlled (24 °C) animal colony under a 12:12-h light/dark cycle with food and water available ad libitum. All behavioral procedures took place during the light cycle. The sodium salt of valproic acid (NaVPA; Sigma-Aldrich) was dissolved in 0.9% saline to obtain a concentration of 150 mg/ml, pH 7.3. Pregnant female SD rats on E12.5 received a single intraperitoneal injection of valproic acid (500 mg/kg), while the control group received 0.9% saline (500 mg/kg) [27]. Dams were housed individually and allowed to raise their own litters until weaning. The VPA-exposed offspring and saline-exposed offspring were housed in cages containing four to five rats until the end of the experiments. All behavioral and electrophysiological experiments were performed on the male offspring at 4–5 weeks of age.

Surgery

Two 22-gauge stainless steel tubes were implanted in the LAs of the male VPA-exposed offspring under ketamine (100 mg/kg, i.p.) and anesthesia. Two cannulas were implanted bilaterally into the LA (anteroposterior, −2.8 mm; mediolateral, ±4.5 mm; dorsoventral, −7.0 mm). The cannulas were fixed to the skull with dental cement. A 28-gauge dummy cannula was inserted into each cannula to prevent clogging. The VPA-exposed offspring were allowed to recover from the surgery for 1 week. DCS (10 μg/side, dissolved in saline) (Abcam) was infused bilaterally into the LA at a rate of 0.1 μl/min, with a volume of 1 μl per side.

Behavioral Testing

A behavioral trace of the rat movements during each experiment was recorded using SMART software (version 3.0; Panlab, S.L.U., Spain).

Three-Chamber Social Interaction Test

The three-chamber social interaction test was adapted from Crawley [28], and performed using 4-week-old saline- and VPA-exposed rat offspring. The test took place in an environment unknown to the rat being tested, in the form of a cage with three communicating compartments. At the beginning of the sociability test, the test rat was placed in the central compartment. In the right compartment (designated "chamber S1"), a stranger rat was placed under a small plastic box (27-cm-long, 13-cm-wide, and 20-cm-high). Stranger rats were randomly selected from saline-exposed rats of the same gender as the test rats. The left compartment, i.e., the empty compartment (designated "chamber E"), had nothing placed in the plastic box. After 5 min, the habituation period, the sociability test was performed for 5 min. The sociability score was defined as the ratio of the time spent time in chamber S1 by the test rat and the whole duration of the examination.

Elevated Plus Maze

The elevated plus maze experiment was used to test for anxiety [29, 30]. The apparatus consisted of four arms (112 × 112 cm), two open and two closed; all arm platforms were elevated 31 cm from the floor. At the start of the trial, the rat was placed in the center of the elevated plus maze and allowed to explore the maze freely. Behavior was observed for 10 min, and the percentage of time spent in the open arms was recorded.

Marble Burying Test

The marble burying test was used to examine obsessive-compulsivity (an anxiety-related behavior) [31]. A clean cage (19 × 10.5 × 8 cm) was prepared with 4-cm corncob bedding material containing 20 embedded marbles. After 20 min, the number of marbles that remained buried in the corncob bedding was recorded.

Brain Slice Preparation and Electrophysiology Recording

The rats were killed by rapid decapitation, and their brains were removed and placed in a beaker containing cold (4 °C) oxygenated (saturated with 95% O_2 and 5% CO_2) sucrose artificial cerebrospinal fluid (ACSF) cutting solution, consisting of (in mM) sucrose 75, NaCl 87, KCl 2.5, $CaCl_2$ 0.5, $MgCl_2$ 4, $NaHCO_3$ 23, NaH_2PO_4 1.25, and glucose 25. Brain slices (400 μm) were prepared using a microslicer (DTK-1000; Dosaka, Kyoto, Japan) and transferred to a recording chamber with normal ACSF, consisting of (in mM) NaCl 130, KCl 2.5, $CaCl_2$ 1.2, $MgCl_2$ 2.4, $NaHCO_3$ 23, NaH_2PO_4 1.2, and glucose 11, and equilibrated with 95% O_2 and 5% CO_2 at 30–32 °C for at least 1 h before use. After a recovery period of 1 h, the slices were transferred to a recording chamber, in which they were continually perfused with oxygenated ACSF (30–32 °C). To record the field excitatory post-synaptic potential (fEPSP) in the lateral amygdala (LA), a concentric bipolar stimulating electrode (FHC, Bowdoinham, ME, USA) was placed in the external capsule and a capillary glass recording electrode (Harvard Apparatus) filled with 3 M NaCl solution was placed in the LA region. The fEPSP was amplified (MultiClamp 700B, Molecular Devices) and digitized (Digidata 1322A, Molecular Devices) for measurement. The stimulation intensity was adjusted to yield a synaptic response of an approximate half-maximal value. Low-frequency stimulation (LFS) producing LTD was elicited by 900 trains of stimuli (1 Hz, 1 s at 1-min intervals) for 15 min at the same stimulation intensity used for the baseline measurements. The chemical LTD induction solution consisted of the above-described ACSF and 20 μM NMDA (Tocris, St. Louis, MO). After 3–5 min of chemical LTD induction, the sections were washed with ACSF for 5 min, and the fEPSPs were monitored for an hour. The paired pulse facilitation (PPF) ratio (second/first fEPSP slope) was measured using two-paired 20-, 40-, 60-, 80-, and 100-ms interpulse interval (IPI) stimuli.

Whole-cell patch-clamp recording from visually identified pyramidal-like neurons located in the LA was performed in a recording chamber with oxygenated ACSF (30–32 °C). Recordings were obtained using a MultiClamp 700B amplifier (Molecular Devices) and Digidata 1322A (Molecular Devices). The recording pipettes (6–6.5 MΩ) were filled with an internal solution containing the following (in mM): 140 K or Cs-gluconate, 10 KCl or CsCl, 1 EGTA, 10 phosphocreatine, 4 Mg-ATP, 0.3 Na-GTP, and 10 HEPES, pH 7.3, 280 mOsm. To isolate miniature excitatory post-synaptic currents (mEPSCs) from the amygdala, we used a K-based internal solution at a holding potential of −70 mV in the presence of tetrodotoxin (1 μM) and picrotoxin (10 μM), which were added to the ACSF. The AMPAR/NMDAR ratio was measured as the ratio of the peak amplitude of the AMPAR-mediated EPSCs recorded at −70 mV and the NMDAR-mediated component of EPSCs recorded at +40 mV. NMDAR-mediated current was determined as amplitude at 50 ms after peak EPSCsamplitude holding at +40 mV.

Western Blotting Analysis

Brain tissues were dissected and lysed in a lysis buffer containing 1% Triton X-100, 0.1% SDS, 50 mM Tris-HCl, pH 7.5, 0.3 M sucrose, 5 mM EDTA, 2 mM sodium pyrophosphate, 1 mM sodium orthovanadate, and 1 m phenylmethylsulfonyl fluoride, supplemented with a complete protease inhibitor cocktail. Following sonication, lysates were centrifuged at 12,000 rpm for 30 min to obtain supernatants. The protein concentrations of the supernatants were measured using a Bradford assay, and equal amounts of protein were separated

by SDS-PAGE electrophoresis, transferred to Immobilon-P membranes (Millipore) and incubated in 5% non-fat dry milk for 60 min. Membranes were incubated with anti-beta actin (1:10,000, Abcam, Cambridge, UK), α-tubulin (1:5000, Cell Signaling Technology, Boston, MA, USA), and anti-AMPA receptor 2 (1:2000, Millipore, Billerica, MA, USA) antibodies overnight at 4 °C, and then incubated with HRP-conjugated secondary antibodies for 1 h at room temperature. Immunoreactivity was detected using ECL Plus detection reagent (PerkinElmer, Boston, MA, USA). Films were exposed for different durations to ensure that the optimum density was achieved without saturation, and this was followed by densitometry. Protein levels were first normalized to the internal control levels for each sample and then measured as the fold change with respect to the control.

Synaptoneurosome Preparation

Synaptoneurosomes were prepared from the amygdala of both the VPA-exposed offspring and the saline-exposed offspring, as described in [32]. Rats were decapitated and the brains were quickly removed and placed on an ice-cold platform for dissection of the amygdala. Isolated amygdala samples were homogenized in 350 μl of ice-cold lysis buffer consisting of 118.5 mM NaC1, 4.7 mM KC1, 1.18 mM $MgSO_4$, 2.5 mM $CaCl_2$, 1.l8 mM KH_2PO_4, 24.9 mM $NaHCO_3$, 10 mM dextrose, and 10 μg/ml adenosine deaminase, with the pH adjusted to 7.4. To minimize proteolysis, proteinase inhibitors (0.01 mg/ml leupeptin, 0.005 mg/ml pepstatin A, 0.1 mg/ml aprotinin, and 5 mM benzamide) were included in the buffer and kept ice cold at all times. This mixture was loaded into a tuberculin syringe attached to a 13-mm-diameter Millipore syringe filter holder. The diluted filtrate was forced over three layers of nylon (Tetko, 100-μm pore size) pre-wetted with 100 μl of synaptoneurosome buffer. The nylon pre-filtered mixture was loaded into another 1-cm^3 tuberculin syringe and forced through a pre-wetted 5-μm Millipore nitrocellulose filter. The filtered particulate was then spun at 1000×*g* for 10 min in a microfuge at 4 °C. The supernatant was removed, and the pellet (synaptoneurosome) was re-suspended in 80 μl of lysis buffer for Western blotting analysis.

Golgi Staining

P28 brain tissues were prepared and processed for Golgi staining using an FD Rapid GolgiStain Kit (FD NeuroTechnologies, Columbia MD, USA) according to the manufacturer's instructions. Briefly, coronal sections of 80 μm in thickness were prepared using microslicer (DTK-1000; Dosaka, Kyoto, Japan) from the amygdala synapses for quantitative analysis. Images were captured using an Olympus BX61 microscope, and spine numbers were counted manually by investigators blind to the experimental conditions.

Statistical Analysis

All values are expressed as the mean ± SEM. The number of animals used is indicated by *n*. The significance of the difference between groups was calculated by one-way ANOVA, two-way ANOVA, and Bonferroni post hoc comparisons to analyze the differences in the results of behavioral tests, electrophysiological responses, spine density, and protein levels between the saline-exposed and VPA-exposed offspring. Correlations between sociability score and inhibition of LTD were analyzed by Pearson's correlation coefficients. Probability values (*p*) of less than 0.05 were considered to represent significant differences.

Results

DCS Rescued Behavioral Abnormalities in VPA-Exposed Offspring

Based on previous studies reporting dysfunction of NMDARs in male VPA-exposed offspring, we reasoned that NMDAR partial agonist DCS might rescue the reduced NMDAR function and ASD-like behaviors observed in the male VPA-exposed offspring. At the age of 4 weeks, DCS (20 mg/kg, i.p.) or saline was administered once per day for 7 days to the male VPA-exposed offspring. Thirty minutes after DCS treatment, the rats were subjected to the three-chamber social interaction test. We found that the impairment in social behavior in the male VPA-exposed offspring was corrected by DCS treatment (Fig. 1a; saline/vehicle $n = 18$, saline/DCS $n = 6$, VPA/vehicle $n = 11$, VPA/DCS $n = 17$; two-way ANOVA revealed the time spent in chamber S1, pre-treatment $F_{(1, 48)} = 5.416$, $p < 0.05$; drug $F_{(1, 48)} = 4.086$, $p < 0.05$; interaction $F_{(1, 48)} = 5.549$, $p < 0.05$; two-way ANOVA revealed the time spent in chamber E, pre-treatment $F_{(1, 48)} = 4.074$, $p < 0.05$; drug $F_{(1, 48)} = 6.573$, $p < 0.05$; interaction $F_{(1, 48)} = 8.862$, $p < 0.01$). The low sociability score was also improved following DCS treatment in the VPA-exposed offspring (Fig. 1b; saline/vehicle $n = 18$, saline/DCS $n = 6$, VPA/vehicle $n = 11$, VPA/DCS $n = 17$; two-way ANOVA, pre-treatment $F_{(1, 48)} = 5.416$, $p < 0.05$; drug $F_{(1, 48)} = 4.086$, $p < 0.05$; interaction $F_{(1, 48)} = 5.549$, $p < 0.05$). To confirm whether DCS local infused bilaterally into the amygdala improves the sociability in VPA-exposed offspring. We administered the DCS (10 μg/side) 30 min in VPA-exposed offspring before three-chamber social interaction test. Similar results were found while infusing with DCS into the amygdala also rescued the social behavior in VPA-exposed offspring (Fig. 1c; saline/vehicle $n = 5$, saline/DCS $n = 5$, VPA/vehicle $n = 5$, VPA/DCS $n = 5$; two-way ANOVA revealed the time spent in chamber S1, pre-treatment $F_{(1, 16)} = 14.57$, $p < 0.01$; drug $F_{(1, 16)} = 8.677$, $p < 0.05$; interaction $F_{(1, 16)} = 18.75$, $p < 0.001$; two-way ANOVA

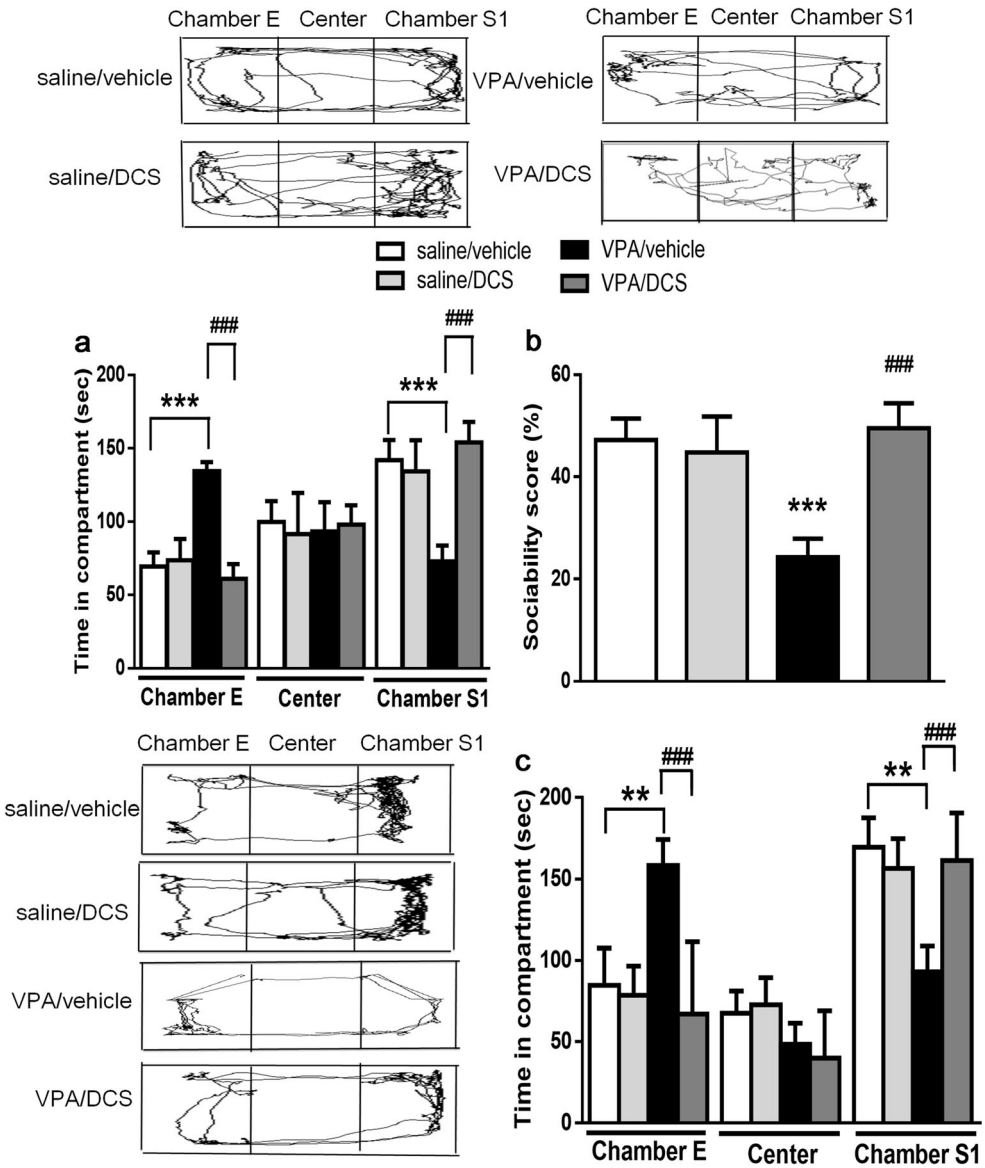

Fig. 1 DCS treatment improved social interaction in the VPA-exposed offspring. **a** Time spent investigating the area of chamber E, center, and chamber S1 during sociability testing in the VPA-exposed offspring with i.p. injection of DCS (20 mg/kg) or saline for 7 days. **b** Bar graphs show the sociability score calculated as time spent in chamber S1/total examination duration in the VPA-exposed offspring with DCS treatment. **c** Bilateral infusion of DCS (10 μg/side) into the amygdala 30 min before three-chamber social interaction test. $^{***}p < 0.001$ vs. saline/vehicle, $^{###}p < 0.001$ vs. VPA/vehicle

revealed the time spent in chamber E, pre-treatment $F_{(1,\ 16)} = 6.344$, $p < 0.05$; drug $F_{(1,\ 16)} = 15.54$, $p < 0.01$; interaction $F_{(1,\ 16)} = 11.81$, $p < 0.01$). In the elevated plus maze (EPM) test, no differences in results were observed between the vehicle- and DCS-treated, saline-exposed offspring; however, DCS administration in the VPA-exposed offspring significantly enhanced the time spent in the open arms in comparison with the vehicle-treated, VPA-exposed offspring (Fig. 2a; saline/vehicle $n = 15$, saline/DCS $n = 6$, VPA/vehicle $n = 19$, VPA/DCS $n = 16$; two-way ANOVA, pre-treatment $F_{(1,\ 52)} = 5.543$, $p < 0.05$; drug $F_{(1,\ 52)} = 11.57$, $p < 0.01$; interaction $F_{(1,\ 52)} = 4.329$, $p < 0.05$). In the marble-burying test of obsessive-compulsive anxiety-like behavior, the VPA-exposed offspring under DCS treatment reversed the burying of more marbles relative to the control rats (Fig. 2b; saline/vehicle $n = 7$, saline/DCS $n = 7$, VPA/vehicle $n = 7$, VPA/DCS $n = 6$; two-way ANOVA, pre-treatment $F_{(1,\ 23)} = 6.423$, $p < 0.05$; drug $F_{(1,\ 23)} = 33.75$, $p < 0.001$; interaction $F_{(1,\ 23)} = 4.781$, $p < 0.05$).

Alteration of Synaptic Plasticity in the Amygdala After DCS Treatment

To confirm the effect of DCS on NMDARs, we isolated NMDAR-mediated EPSCs evoked by electrical stimulation at a holding potential of +40 mV in the presence of CNQX (40 μM) and picrotoxin (100 μM). After application of DCS (10 μM) to the amygdala synapses, the mean peak amplitude of the evoked NMDAR-mediated EPSCs increased from 100.9 ± 0.86 to 144.6 ± 5.739 pA (Fig. 3a; $n = 4$). We have previously shown that VPA-exposed offspring of 4–5 weeks of age exhibited impaired NMDAR-dependent LTD in the amygdala synapses [26]. We examined the effect of DCS on the NMDAR-dependent LTD in the amygdala synapses in the

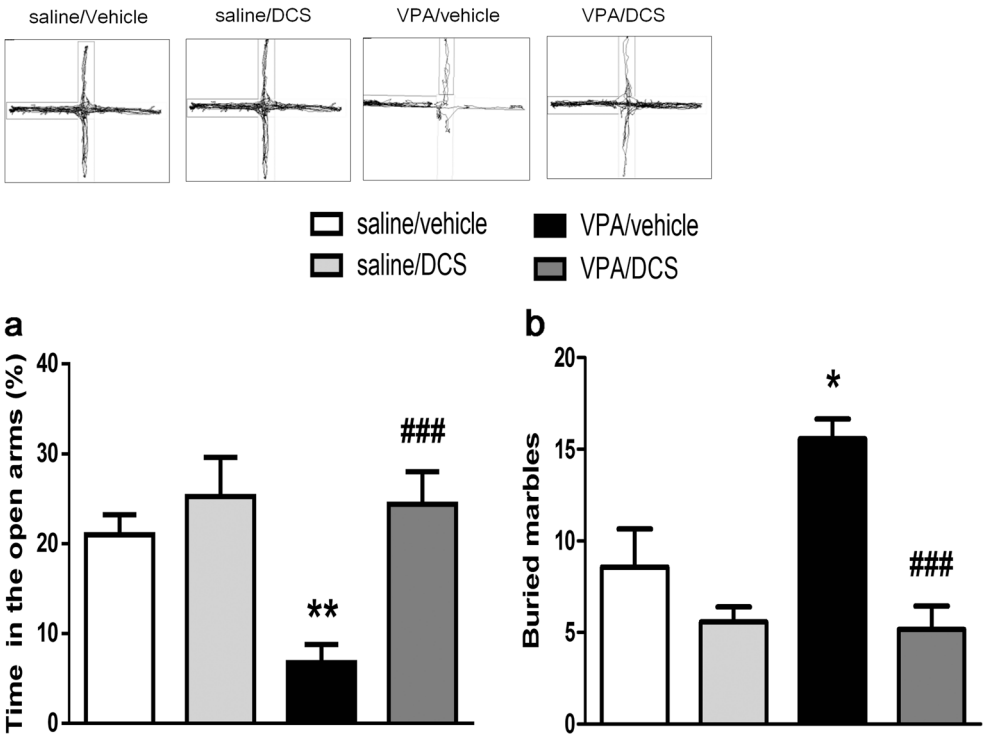

Fig. 2 DCS ameliorated anxiety/repetitive-like behaviors in the VPA-exposed offspring. **a** Bar chart showing the percentage of time spent in the open arms after administration of DCS (20 mg/kg) or saline for 7 days in the VPA-exposed offspring. **b** Bar chart showing the number of buried marbles in the VPA-exposed offspring with DCS treatment. *$p < 0.05$ vs. saline/vehicle, **$p < 0.01$ vs. saline/vehicle, ### $p < 0.001$ vs. VPA/vehicle

4–5-week-old VPA-exposed offspring. The results revealed that chronic treatment with DCS for 7 days reversed the impaired NMDAR-dependent LTD in the VPA-exposed offspring (Fig. 3b; saline 61.08 ± 5.63% of baseline, $n = 5$; VPA 97.83 ± 1.18% of baseline, $n = 4$; VPA/vehicle 95.43 ± 1.48% of baseline, $n = 5$; VPA/DCS 65.83 ± 1.79% of baseline, $n = 6$). Similar results also showed that DCS rescued the deficit in chemical LTD induced by NMDA in the amygdala of the VPA-exposed offspring (Fig. 3c; saline 68.90 ± 5.57% of baseline, $n = 4$; VPA 95.18 ± 2.32% of baseline, $n = 3$; VPA/vehicle 101.20 ± 1.99% of baseline, $n = 4$; VPA/DCS 75.87 ± 4.33% of baseline, $n = 4$). Figure 3d compares the effect of DCS on LFS- ($F_{(3,\ 16)} = 10.64$, $p < 0.01$) and chemical NMDA-induced LTD ($F_{(3,\ 11)} = 17.52$, $p < 0.01$) in the amygdala of the VPA-exposed offspring. Additionally, we further compared the relationship between sociability and inhibition of LTD. We found that the sociability score was positively correlated with LTD inhibition, suggesting that the social impairment further influence the synaptic plasticity of LTD in VPA-exposed offspring (Fig. 3e; $r = 0.679$, $p < 0.001$).

DCS Rescued the Increase in Spine Density in the Amygdala of VPA-Exposed Offspring

The density and morphology of dendritic spines change in accordance with long-term synaptic plasticity [33, 34]. We found that the DCS treatment did not alter the spine density in the saline-exposed offspring (Fig. 4a; 0.3627 ± 0.031 spine/μm, $n = 5$, $p = 0.77$). We thus analyzed the effects of DCS treatment on alterations in the amygdala spine density of the VPA-exposed offspring. Compared with the saline-exposed offspring (0.372 ± 0.008 spine/μm, $n = 5$, $p < 0.01$), the spine densities were found to be greater in the amygdala of VPA-exposed offspring (0.4799 ± 0.019 spine/μm, $n = 5$); however, after chronic DCS treatment for 7 days, we observed a decreased spine density in the VPA-exposed offspring (Fig. 4a; 0.3808 ± 0.009 spine/μm, $n = 4$, $p < 0.05$). We next evaluated whether the enhancement in spine density in the VPA-exposed offspring was accompanied by a functional enhancement in excitatory synaptic transmission. Using whole-cell voltage clamp recordings to assess mEPSCs in the amygdala, we observed significant increases in the mEPSC amplitude and frequency in the VPA-exposed offspring, and DCS application reversed the increased amplitude ($F_{(3,\ 12)} = 9.474$, $p = 0.017$) and frequency ($F_{(3,\ 12)} = 5.984$, $p = 0.009$) of mEPSC in the VPA-exposed offspring (Fig. 4b,c). We further analyzed the PPF; the VPA-exposed offspring had significantly decreased PPF ratios at interpulse intervals of 20 ms (1.010 ± 0.029, $n = 5$) and 40 ms (0.996 ± 0.031, $n = 5$) in comparison to the saline-exposed offspring (20 ms 1.220 ± 0.023, $n = 12$, $p < 0.01$; 40 ms 1.179 ± 0.015, $n = 12$, $p < 0.01$). However, administration of DCS reversed the difference in PPF ratio, leading to a level comparable to that of the saline-exposed offspring (Fig. 4d; 20 ms 1.263 ± 0.042, $n = 12$, $p < 0.05$; 40 ms 1.199 ± 0.029, $n = 12$, $p < 0.05$). The results suggested that DCS normalized the synaptic function in the amygdala of the VPA-exposed offspring.

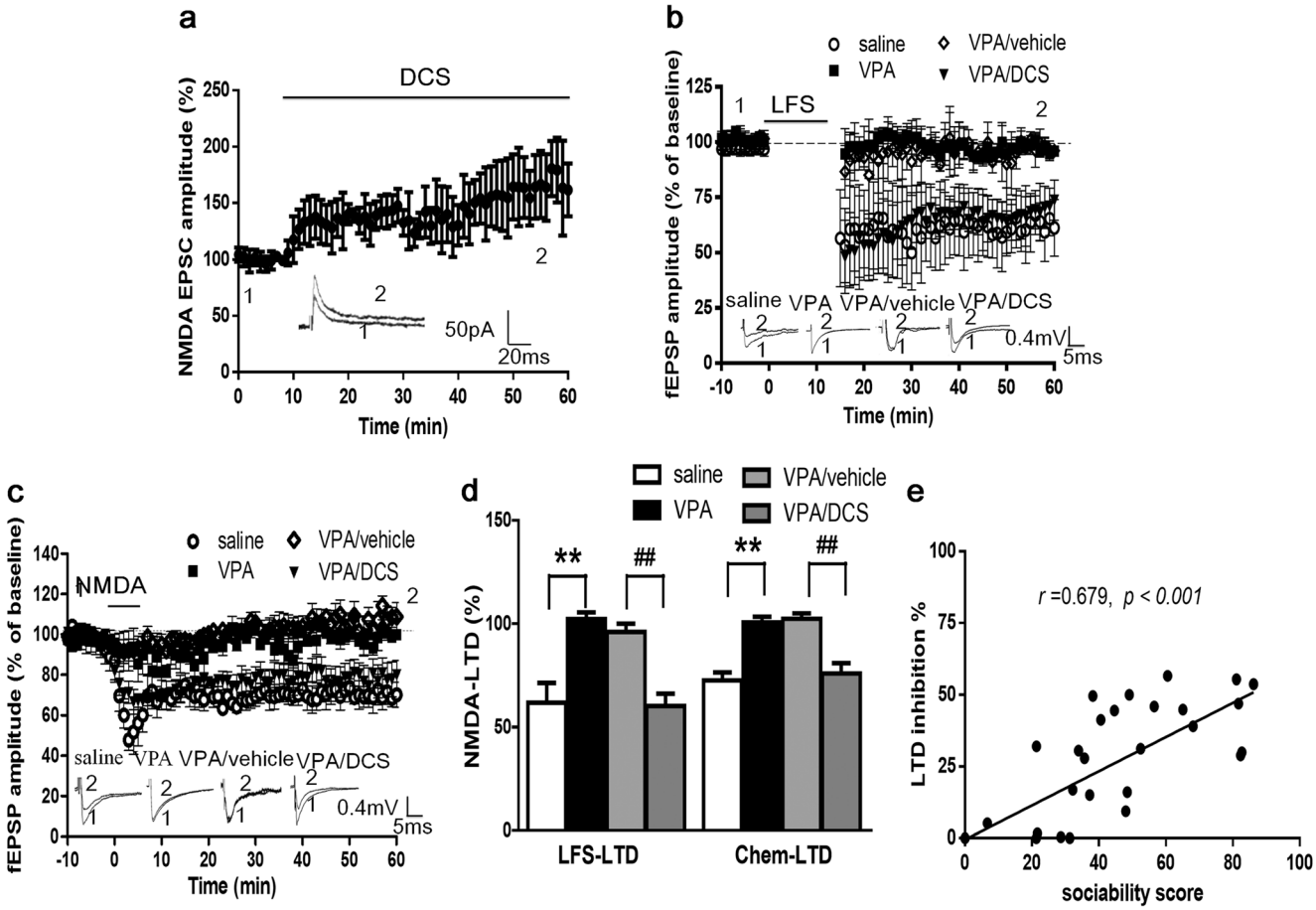

Fig. 3 Reversal of NMDA receptor-dependent, long-term synaptic depression (NMDA-LTD) by DCS in the VPA-exposed offspring. **a** In an experiment performed with neurons from 4- to 6-week-old rats, application of DCS (10 μM) enhanced the amplitude of NMDA EPSCs. **b** Experiments showed that LFS (1 Hz, 15 min) did not produce LTD, which was reversed by DCS treatment. **c** Experiments showed that chemical NMDA (20 μM) did not induce LTD, which was reversed by DCS treatment. **d** Bar chart comparing the effects of LFS- and chemical NMDA-induced LTD with DCS treatment in the VPA-exposed offspring. **e** Correlation between sociability score and LTD inhibition percent. $^{**}p < 0.01$ vs. saline, $^{\#\#}p < 0.01$ vs. VPA/vehicle

DCS Enhanced Synaptic Removal of GluA2/AMPARs During LTD in the Amygdala of VPA-Exposed Offspring

GluA2/AMPARs have been proposed to play a dominant role in the activity-dependent endocytosis of AMPARs associated with LTD [35–38]. Using Western blotting of synaptoneurosomes from acute slices of the rat amygdala, we examined whether DCS enhanced LFS-induced LTD of GluA2/AMPAR removal in the VPA-exposed offspring. As shown in Fig. 5a, LFS (1 Hz for 15 min) did not significantly alter the surface expression of GluA2/AMPARs in the VPA-exposed offspring (70.00 ± 7.071%, $n = 4$) as compared with the saline-exposed offspring (50.00 ± 9.256%, $n = 4$). ANOVA indicated a main effect of group ($F_{(4, 15)} = 11.84$; $p < 0.001$), with the DCS treatment group showing lower GluA2/AMPAR levels than the group of VPA-exposed offspring without DCS treatment. Similar results were observed for NMDA-induced chemical LTD; NMDA (20 μM) application did not influence the surface expression of GluA2/AMPARs in the VPA-exposed offspring (99.00 ± 11.500%, $n = 7$) as compared with the saline-exposed offspring (62.88 ± 8.166%, $n = 7$). DCS reversed the increased GluA2/AMPAR level after NMDA application in the VPA-exposed offspring (Fig. 5b; $F_{(4, 27)} = 6.579$, $p < 0.001$).

$GluA2_{3Y}$ Blocked the Effects of DCS Facilitation of Synaptic Removal of GluA2/AMPARs During LTD and Sociability in the VPA-Exposed Offspring

Previous studies have shown that short C-terminal sequences of GluA2/AMPAR subunits are critical for regulating AMPAR endocytosis during hippocampal LTD [38]. A synthetic peptide containing a GluA2/AMPAR carboxyl tail ($GluA2_{3Y}$; $_{869}$YKEGYNVYG$_{877}$) has been shown to block AMPAR endocytosis in the hippocampus and amygdala [38, 39]. We next explored interference with the activity-dependent synaptic removal of GluA2/AMPARs during NMDA-induced chemical LTD. We analyzed by Western blotting synaptoneurosomes from slices incubated with Tat-$GluA2_{3Y}$ (10 μM) or a control peptide Tat-$GluA2_{3A}$ ($_{869}$AKEGYNVYG$_{877}$) for 30 min before application of DCS (10 μM) in the VPA-exposed offspring. The

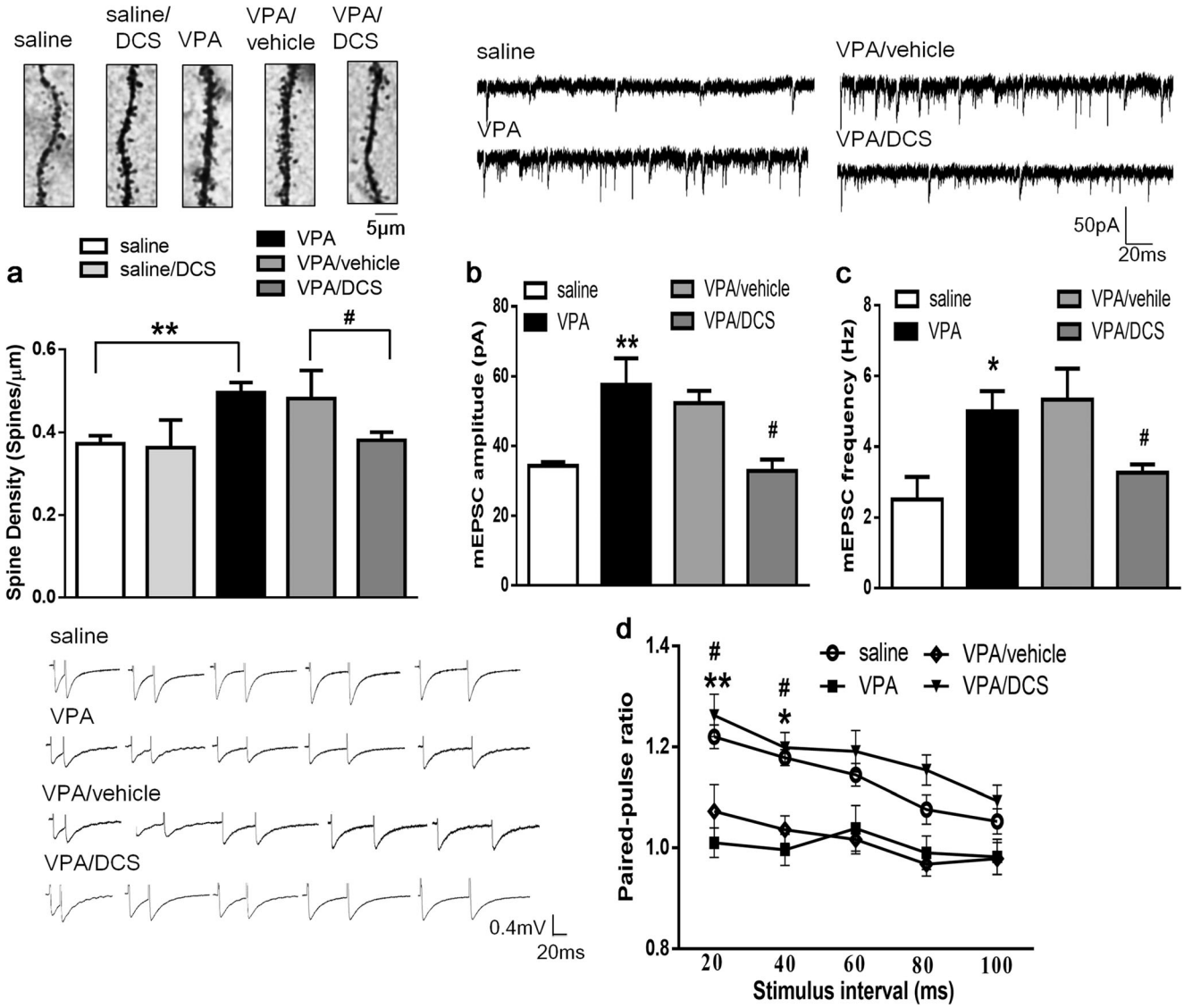

Fig. 4 Effects of DCS on mEPSCs and short-term plasticity in the VPA-exposed offspring. **a** Representative Golgi-stained sections of spines in the lateral amygdala (LA) are shown (scale bar indicates 5 μm). **b** Amplitudes of mEPSCs were recorded in LA neurons at a holding potential of −70 mV in the presence of TTX (1 μM) and picrotoxin (10 μM). **c** Frequencies of mEPSCs were recorded in LA neurons at a holding potential of −70 mV in the presence of TTX (1 μM) and picrotoxin (10 μM). **d** Comparison of paired-pulse ratios (PPRs) of fEPSPs in the LA synapses after DCS treatment in the VPA-exposed offspring. $^{*}p < 0.05$ vs. saline, $^{**}p < 0.01$ vs. saline, $^{\#}p < 0.05$ vs. VPA/vehicle, $^{*}p < 0.05$ vs. saline, $^{**}p < 0.01$ vs. saline, $^{\#}p < 0.05$ vs.VPA/vehicle

results showed that Tat-GluA2$_{3Y}$ blocked the facilitative effect of DCS on GluA2/AMPAR removal during NMDA-induced chemical LTD (119.3 ±4.1%, $n = 4$), whereas treatment with inactive Tat-GluA2$_{3A}$ failed to affect the expression of GluA2/AMPARs in the VPA-exposed offspring (Fig. 6a; 84.75 ± 6.651%, $n = 4$). We also examined whether Tat-GluA2$_{3Y}$ altered the AMPA/NMDA ratio after DCS treatment in the VPA-exposed offspring. There was no difference in the AMPA/NMDA ratio between the VPA, VPA/DCS, and VPA/DCS/Tat-GluA2$_{3Y}$ groups (Fig. 6b; $F_{(2,\ 13)} = 0.891$, $p = 0.433$). Furthermore, Tat-GluA2$_{3Y}$ blocked the effect of DCS reversed the increased spine density (0.4331 ± 0.015 spine/μm, $n = 4$, $p < 0.01$), whereas the inactive Tat-GluA2$_{3A}$ failed to influence the effect of DCS on spine density in amygdala of VPA-exposed offspring (Fig. 6c; 0.303 ± 0.021 spine/μm, $n = 4$, $p < 0.01$).

In a battery of behavioral tests, we performed the three-chamber social interaction test to determine whether Tat-GluA2$_{3Y}$ influenced the effect of DCS on social behaviors of the VPA-exposed offspring. We administrated Tat-GluA2$_{3Y}$ (3 μmol/kg i.p.) or Tat-GluA2$_{3A}$, followed by DCS (20 mg/kg, i.p.) or vehicle 1 h before sociability testing. The results showed that DCS increased the time spent in the social zone; this sociability increase was blocked by Tat-GluA2$_{3Y}$ administration (time in social zone 80.23 ± 11.06 s, $n = 6$; sociability score 26.74 ± 3.687%, $n = 6$) as compared with the Tat-GluA2$_{3A}$ group (time in social zone 136.6 ± 9.851 s, $n = 4$,

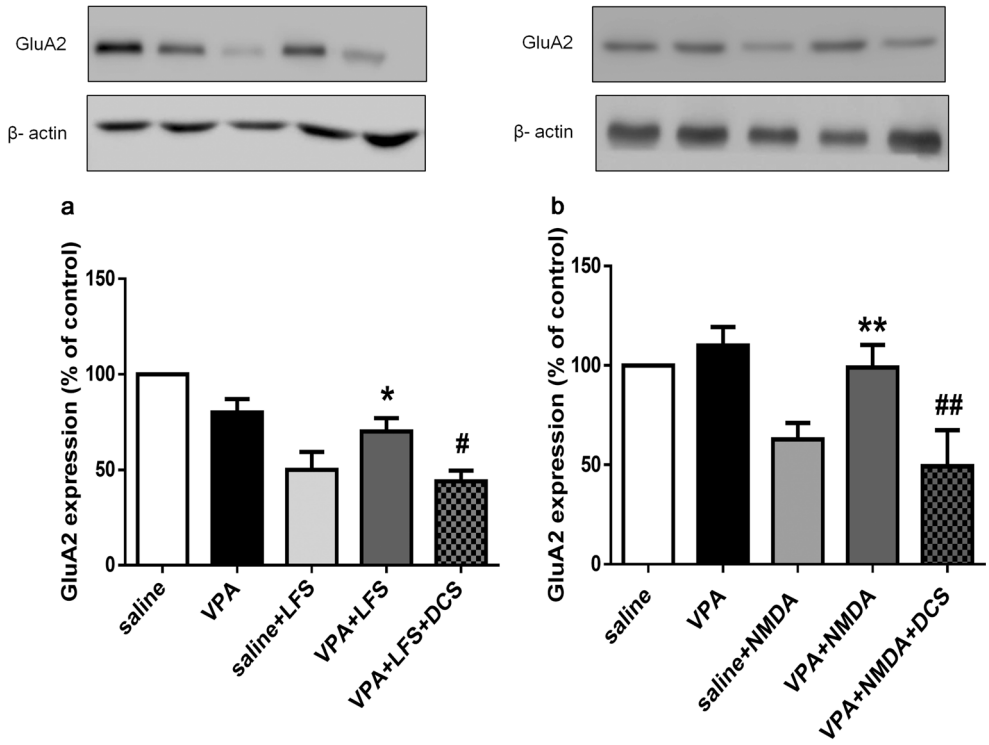

Fig. 5 DCS reversed the impaired GluA2/AMPAR removal after induction of NMDA-dependent LTD in the amygdala of VPA-exposed offspring. **a** Immunoblots and quantification showing the cytosolic fraction of synapses after LFS-induced removal of GluA2/AMPARs in the LA of VPA-exposed offspring with DCS treatment. **b** Immunoblots and quantification showing the cytosolic fraction of synapses after chemical NMDA-induced removal of GluA2/AMPARs in the LA of VPA-exposed offspring with DCS treatment. $^{*}p < 0.05$ vs. saline + LFS, $^{\#}p < 0.05$ vs. VPA + LFS, $^{**}p < 0.01$ vs. saline + NMDA, $^{\#\#}p < 0.01$ vs. VPA + NMDA

$p < 0.05$; sociability score 45.52 ± 3.284%, $n = 4$, $p < 0.05$), indicating that Tat-GluA2$_{3Y}$ specifically disrupted the effect of DCS in terms of improving social behavior in the VPA-exposed offspring (Fig. 7a,b). Furthermore, we also analyzed that the effect of Tat-GluA2$_{3Y}$ interferes DCS on GluA2/AMPAR removal in VPA-exposed offspring . We found that the effect of DCS facilitation GluA2/AMPAR would be blocked by Tat-GluA2$_{3Y}$ (109.1 ± 3.263% $n = 5$), whereas the Tat-GluA2$_{3A}$ did not influence the expression of GluA2/AMPARs in the VPA-exposed offspring (Fig. 7c; 81.33 ± 1.856%, $n = 5$).

Discussion

In the present study, we found that DCS improved social interaction and anxious behavior in the VPA-exposed offspring. The observation of reversal of impaired NMDAR-dependent LTD and enhanced spine density coupled with increased mEPSCs and PPF by DCS treatment in the amygdala of the VPA-exposed offspring suggested that the synaptic plasticity underlies the behavioral abnormality in this model of ASD. Exploring the functional role of GluA2/AMPAR internalization in LTD, we found that Tat-GluA2$_{3Y}$ disrupted the DCS-rescued, NMDAR-dependent LTD in the VPA-exposed offspring. Thus, these results suggested that DCS rescued the autistic patterns in a VPA-induced autism model, which was mediated by the regulation of activity-dependent removal of GluA2/AMPARs in the amygdala synapses.

The amygdala complex is the site of neural circuitry. Socio-emotional behavior is affected by both genetic and non-genetic factors in ASD [40, 41]. Defects in the amygdala have been suggested to disrupt information processing within the amygdala and between the amygdala and connected brain regions, causing abnormal ASD-like behavior patterns [42, 43]. Previous studies found enhanced excitability, which further resulted in excitatory/inhibitory (E/I) imbalance in the amygdala of VPA-exposed offspring [44, 45]. Furthermore, enhanced anxiety and fear processing in the amygdala of VPA-exposed offspring result in withdrawal from social interaction [46]. Our previous study revealed dysfunction of NMDARs in the amygdala of VPA-exposed offspring, which suggested abnormality of the amygdala resulting deficits in synaptic function and ASD-like behaviors [26].

NMDAR dysfunction has been implicated to contribute to ASD. Clinical studies of ASD have identified a do novo mutation in *GRIN2B* [47–49]. In addition, single-nucleotide polymorphism analysis also linked *GRIN2A* and *GRIN2B* to the ASD [50]. The elevated NMDAR function shown in the ASD model of *IRSp53*$^{-/-}$ mice could be improved by application of memantine, an NMDAR antagonist [9]. *Shank2*$^{-/-}$ mice showed decreased NMDAR function, and DCS administration normalized NMDARs and improved social interaction [8]. Alteration of NMDAR function may disturb downstream processes, including synaptic plasticity, E/I balance, and AMPAR trafficking, which induce ASD-like disorders [51, 52]. Furthermore, alterations in glycinergic signaling have been reported to regulate the social and cognitive impairments in non-syndromic ASD [53]. In agreement with this, we found that impairment of NMDAR-

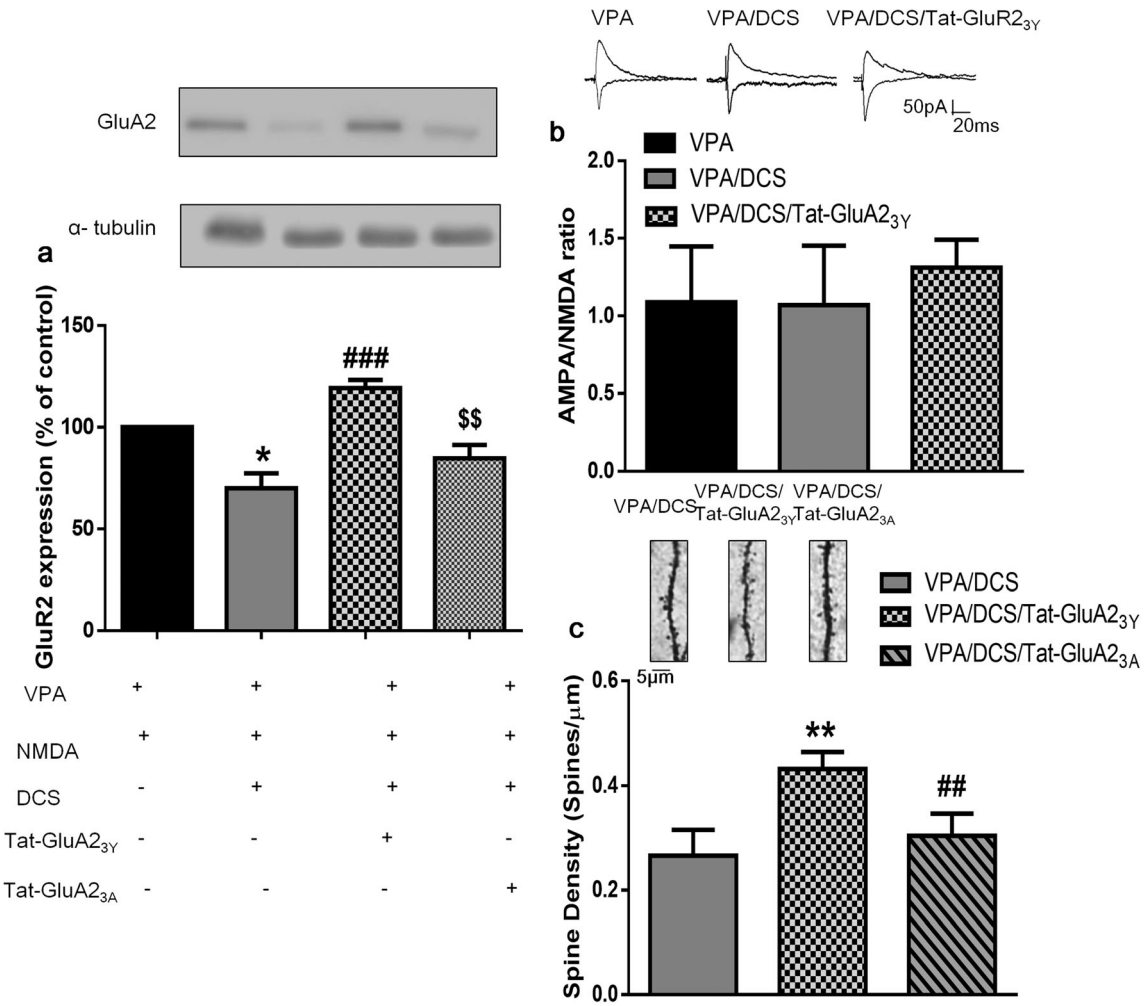

Fig. 6 Tat-GluA2$_{3Y}$ blocked DCS-rescued, NMDA-induced removal of GluA2/AMPARs in VPA-exposed offspring. **a** Immunoblots and quantification showing that Tat-GluA2$_{3Y}$ (10 μM) blocked the effect of DCS (10 μM), facilitating chemical NMDA-induced removal of GluA2/AMPARs in the LA of VPA-exposed offspring. **b** Bar chart showing the AMPA/NMDA ratio in the VPA-exposed offspring injected with DCS and Tat-GluA2$_{3Y}$. The result was calculated as the ratio of the AMPAR-mediated EPSC amplitudes recorded −70 mV and the NMDAR-mediated component of EPSCs recorded at +40 mV. **c** Representative Golgi-stained sections of the Tat-GluA2$_{3Y}$ that blocked the effect of DCS reversed the increased spines in the amygdala of VPA-exposed offspring (scale bar indicates 5 μm). *$p < 0.05$ vs. VPA + NMDA, **$p < 0.01$ vs. VPA/DCS, $^{\#\#}p < 0.01$ vs. VPA/DCS/Tat-GluA2$_{3Y}$, $^{\#\#\#}p < 0.001$ vs. VPA + NMDA + DCS, $^{\$\$}p < 0.01$ vs. VPA + NMDA + DCS + Tat-GluA2$_{3Y}$

dependent LTD could be rescued by DCS, which acts at the glycine site on NMDARs in the amygdala of VPA-exposed offspring. The reason for there being no significant differences in the AMPA/NMDA ratio, a result similar to that of a previous study [44], is not yet known, but may be attributed to AMPAR involvement in this study. Our data showed that DCS decreases the mEPSCs in the VPA-exposed offspring, which represented that the DCS decreases the AMPA-mediated EPSC amplitudes in recording −70 mV. It is similar with the previous study that reported that DCS depresses AMPA/kainate receptor-mediated synaptic responses [24]. The enhanced NMDAR function of VPA-exposed offspring has been reported in the previous studies [54, 55]. DCS is known as a positive modulator to enhance NMDAR function. However, DCS has been recently reported to negatively modulate the excessive activation of NMDAR in ischemic stroke and traumatic brain injury animal models [56, 57]. As a modulator, we speculate that DCS may modulate and decrease the NMDAR function in VPA-exposed offspring. Therefore, we thought that the AMPA/NMDA ratio did not change, owing to reduce both the AMPA and NMDA currents in VPA-exposed offspring. The detailed mechanism of DCS involved in regulating the AMPAR and NMDAR in VPA-exposed offspring merits further investigation.

NMDAR has been reported as the coincidence of synaptic plasticity expressed while changes the AMPAR-mediated transmission by alternating the insertion or removal of AMPAR subunits [58, 59]. NMDARs promote the insertion of GluA1/AMPARs into synapses, leading to synaptic potentiation or removal of GluA1/AMPARs and GluA2/AMPARs from synapses, causing synaptic depression [60, 61]. In vivo studies have

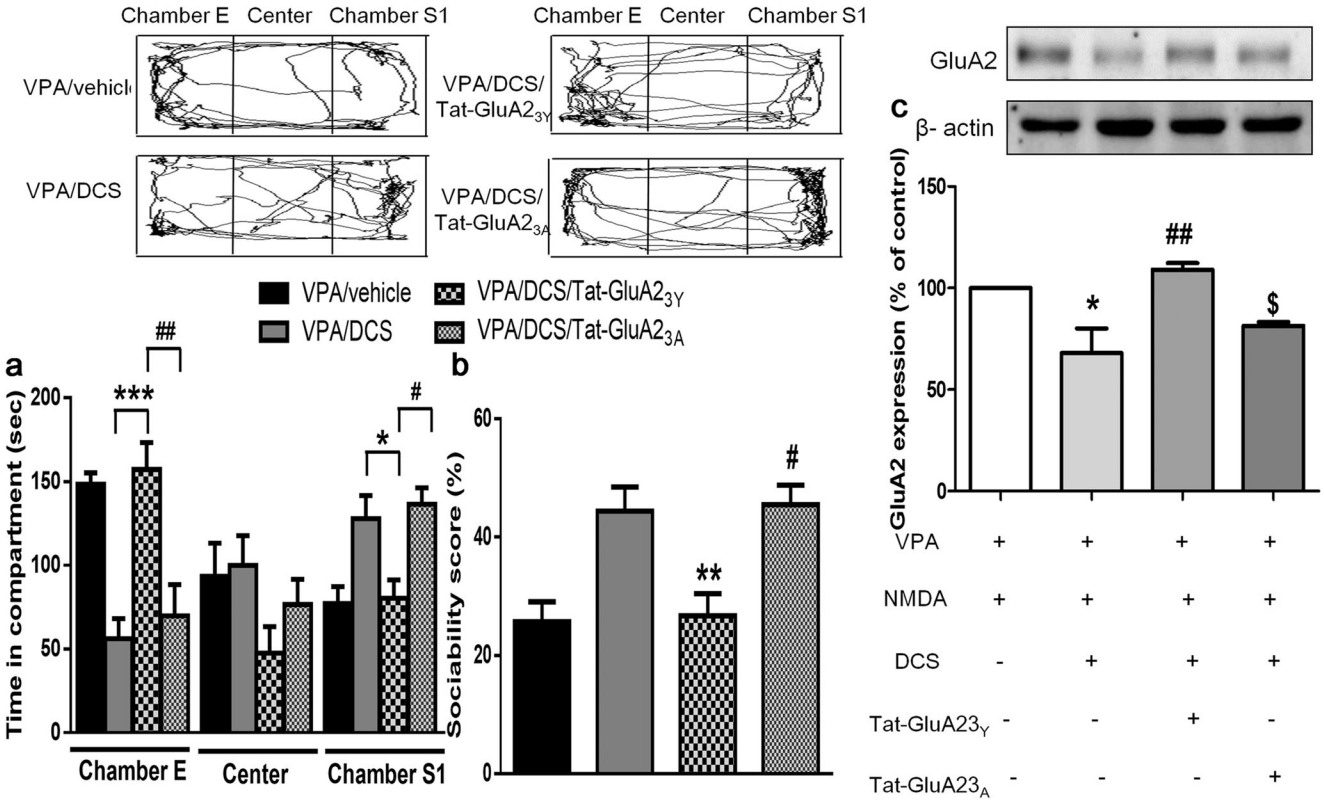

Fig. 7 Tat-GluR2$_{3Y}$ disrupted the effect of DCS on sociability improvement in VPA-exposed offspring. **a** Time spent investigating the area of chamber E, center, and chamber S1 during sociability testing in the DCS-treated, VPA-exposed offspring with administration of Tat-GluA2$_{3Y}$ (3 μmol/kg i.p.) and Tat-GluA2$_{3A}$. **b** Bar chart showing the sociability score in DCS-treated, VPA-exposed offspring with administration of Tat-GluA2$_{3Y}$ and Tat-GluA2$_{3A}$. **c** Immunoblots and quantification showing that Tat-GluA2$_{3Y}$ (3 μmol/kg i.p) blocked the effect of DCS (20 mg/kg), facilitating chemical NMDA-induced removal of GluA2/AMPARs in the LA of VPA-exposed offspring. $^{*}p < 0.05$ vs. VPA + NMDA + DCS, $^{**}p < 0.01$ vs. VPA/DCS, $^{***}p < 0.001$ vs. VPA/DCS, $^{\#}p < 0.05$ vs. VPA/DCS/Tat-GluA2$_{3Y}$, $^{\#\#}p < 0.01$ vs. VPA + NMDA + DCS, $^{\$}p < 0.01$ vs. VPA + NMDA + DCS + Tat-GluA2$_{3Y}$

shown altered AMPAR trafficking in the pathogenic mechanism of ASD, including a lack of activity-dependent synaptic trafficking of GluA1, in *Mecp2* KO mice [62, 63]. Furthermore, the glutamate receptor interacting protein (GRIP), a major scaffolding protein for AMPAR subunits GluA2/3 that regulates surface expression, receptor trafficking, and several forms of synaptic plasticity, has been implicated in the modulation of autistic phenotypes, while double knockout of Grip1/2 in mice reduced surface AMPARs and prevented upregulation of surface AMPARs or synaptic strength [64–66]. Furthermore, the Grip1/2-mediated AMPAR signaling has also been reported to increase social behaviors [65, 66]. We found, in the VPA-exposed offspring, that trafficking of GluA2/AMPARs in the synapses was lacking after NMDAR-dependent LTD. Therefore, we predicted that alteration of GRIP in the amygdala synapses may also lead to impaired synaptic plasticity and ASD phenotypes in VPA-exposed offspring.

To determine whether the absence of trafficking of GluA2/AMPARs in synapses drives autistic phenotypes in VPA-exposed offspring, we administrated AMPAR endocytosis-interfering peptide Tat-GluA2$_{3Y}$ to the amygdala synapses. Our finding that the effects of DCS in terms of rescuing LTD and restoring the AMPAR trafficking were disrupted by Tat-GluA2$_{3Y}$ clearly indicated that the DCS reversed abnormality in synaptic plasticity was mediated by GluA2/AMPARs. This was consistent with a previous report demonstrating that DCS enabled LTD-induced internalization of GluA1/AMPARs and GluA2/AMPARs in the amygdala synapses [25]. In addition, Tat-GluA2$_{3Y}$ also blocked the sociability improvement resulting from DCS treatment. In corroboration with our results, the impaired social interaction induced by NMDAR antagonists was prevented by Tat-GluA2$_{3Y}$ [67]. These data suggested that impaired endocytosis of GluA2/AMPARs contributed to the ASD phenotype, and DCS reversal of synaptic plasticity and behaviors may be mediated by GluA2/AMPAR trafficking, providing another molecular target for ASD treatment.

The ASD human brain revealed an increase in spine density of pyramidal neurons from temporal and parietal lobes, suggesting that there exists an inverse relationship between spine density and cognitive function [68]. Previous study identified that loss of NMDAR subunit NR1 decrease spine density and increased spine head size in the developing cortex, suggesting that NMDARs regulate synapse structure and

function [69]. In addition, knockdown of NMDARs resulted in unstable spines, indicating the importance of NMDARs for spine stability [70]. Furthermore, SAP102, which links NMDA subunit NR2B, also regulates the length of dendritic spines [71]. Based on the results of previous and current studies, we speculated that dysfunction of NMDARs further results in abnormality of spine density in the amygdala synapses of VPA-exposed offspring [26, 44]. However, whether the dysfunction of NMDARs alters the motility of dendritic spines in amygdala neurons of VPA-exposed offspring needs further investigation. Recent evidence suggested that abnormality in spine development in GluD1 KO mice was corrected by modulation of NMDAR function by DCS [72]. Similarly, in our study, we found that DCS reversed the increase in spine density in the amygdala of the VPA-exposed offspring. Profilin, an actin polymerization-regulatory protein, has been reported to increase translocation into the amygdala synapses of dendritic spines after fear conditioning [73]. A previous study also identified enhancement of dendritic spines following fear conditioning in rodents [74]. Enhancement of fear learning related to the amygdala has been established in VPA-exposed offspring and hence is probably the reason for which the spine density increased in the amygdala synapses without any other neuronal or synaptic stimulation in the VPA-exposed offspring [44, 46]. Cofilin activity has been shown to regulate the growth and shrinkage of dendritic spines; however, the role of signaling of Rac1/PAK/cofilin in the amygdala of VPA-exposed offspring requires further study [75]. Alteration of the spine density has an impact on the amount of excitatory neurotransmission; in addition, amygdala pyramidal neurons have shown a deficit in inhibition, which has been considered the reason for E/I imbalance in VPA-induced offspring [46, 76]. Indeed, we also observed increases in the frequency and amplitude of mEPSCs consistent with ASD imbalance between excitatory/inhibitory synaptic transmissions. After DCS restoral of NMDAR function, the excitatory synaptic transmission in the amygdala of the VPA-exposed offspring was reduced.

In summary, the mechanism of DCS rescue of deficits in a VPA-induced ASD model via facilitation of GluA2/AMPAR internalization suggested that the modulation of GluA2/AMPARs is a potential approach for improvement of ASD.

Acknowledgments The authors would like to thank OxBioSci for editing the English in this manuscript and all of the research participants. This study was supported by grants MOST 105-2628-B-010-006–MY3, MOST 104-2314-B-006-030-MY3, MOST 103-2321-B-010-016, and MOST 99-2628-B-006-013-MY3 from the Ministry of Science and Technology of Taiwan. This study was also supported by Yen Tjing Ling Medical Foundation, Taiwan (CI-105-12); National Yang-Ming University-Far Eastern Memorial Hospital Joint Research Program (#NYMU-FEMH 106DN09); the Brain Research Center, National Yang-Ming University; and a grant from Ministry of Education, Aim for the Top University Plan, Taiwan. The funding institutions of this study had no further role in the study design, the collection, analysis, and interpretation of data; the writing of this paper; or the decision to submit it for publication.

Authors' Contributions HC Lin and PS Chen conceived and designed the experiments. HF Wu, YT Hsu, CW Lee, TF Wang, and YJ Chen performed the experiments. HF Wu and PS Chen analyzed the data. PS Chen contributed reagents/materials/analysis tools. HF Wu and HC Lin wrote the paper.

Compliance with Ethical Standards

Conflict of Interest The authors declare that they have no conflicts of interest.

References

1. Rodier PM, Ingram JL, Tisdale B, Nelson S, Romano J (1996) Embryological origin for autism: developmental anomalies of the cranial nerve motor nuclei. J Comp Neurol 370(2):247–261. doi:10.1002/(SICI)1096-9861(19960624)370:2<247::AID-CNE8>3.0.CO;2-2
2. Rapin I, Tuchman RF (2008) Autism: definition, neurobiology, screening, diagnosis. Pediatr Clin N Am 55(5):1129–1146, **viii**. doi:10.1016/j.pcl.2008.07.005
3. Ratajczak HV (2011) Theoretical aspects of autism: causes—a review. J Immunotoxicol 8(1):68–79. doi:10.3109/1547691X.2010.545086
4. Lee EJ, Lee H, Huang TN, Chung C, Shin W, Kim K, Koh JY, Hsueh YP et al (2015) Trans-synaptic zinc mobilization improves social interaction in two mouse models of autism through NMDAR activation. Nat Commun 6:7168. doi:10.1038/ncomms8168
5. Rubenstein E, Wiggins LD, Lee LC (2015) A review of the differences in developmental, psychiatric, and medical endophenotypes between males and females with autism spectrum disorder. J Dev Phys Disabil 27(1):119–139. doi:10.1007/s10882-014-9397-x
6. Werling DM, Geschwind DH (2013) Sex differences in autism spectrum disorders. Curr Opin Neurol 26(2):146–153. doi:10.1097/WCO.0b013e32835ee548
7. Sztainberg Y, Zoghbi HY (2016) Lessons learned from studying syndromic autism spectrum disorders. Nat Neurosci 19(11):1408–1417. doi:10.1038/nn.4420
8. Won H, Lee HR, Gee HY, Mah W, Kim JI, Lee J, Ha S, Chung C et al (2012) Autistic-like social behaviour in Shank2-mutant mice improved by restoring NMDA receptor function. Nature 486(7402):261–265. doi:10.1038/nature11208
9. Chung W, Choi SY, Lee E, Park H, Kang J, Choi Y, Lee D, Park SG et al (2015) Social deficits in IRSp53 mutant mice improved by NMDAR and mGluR5 suppression. Nat Neurosci 18(3):435–443. doi:10.1038/nn.3927
10. Meldrum B, Garthwaite J (1990) Excitatory amino acid neurotoxicity and neurodegenerative disease. Trends Pharmacol Sci 11(9):379–387
11. Hofmann SG, Wu JQ, Boettcher H (2013) D-cycloserine as an augmentation strategy for cognitive behavioral therapy of anxiety disorders. Biol Mood Anxiety Disorders 3(1):11. doi:10.1186/2045-5380-3-11
12. Davis M (2011) NMDA receptors and fear extinction: implications for cognitive behavioral therapy. Dialogues Clin Neurosci 13(4):463–474
13. van Berckel BN, Evenblij CN, van Loon BJ, Maas MF, van der Geld MA, Wynne HJ, van Ree JM, Kahn RS (1999) D-cycloserine increases positive symptoms in chronic schizophrenic patients when administered in addition to antipsychotics: a double-blind, parallel, placebo-controlled study. Neuropsychopharmacology : official

publication of the American College of Neuropsychopharmacology 21(2):203–210. doi:10.1016/S0893-133X(99)00014-7
14. Ren J, Li X, Zhang X, Li M, Wang Y, Ma Y (2013) The effects of intra-hippocampal microinfusion of D-cycloserine on fear extinction, and the expression of NMDA receptor subunit NR2B and neurogenesis in the hippocampus in rats. Prog Neuro-Psychopharmacol Biol Psychiatry 44:257–264. doi:10.1016/j.pnpbp.2013.02.017
15. Posey DJ, Kem DL, Swiezy NB, Sweeten TL, Wiegand RE, McDougle CJ (2004) A pilot study of D-cycloserine in subjects with autistic disorder. Am J Psychiatry 161(11):2115–2117. doi:10.1176/appi.ajp.161.11.2115
16. Urbano M, Okwara L, Manser P, Hartmann K, Herndon A, Deutsch SI (2014) A trial of D-cycloserine to treat stereotypies in older adolescents and young adults with autism spectrum disorder. Clin Neuropharmacol 37(3):69–72. doi:10.1097/WNF.0000000000000033
17. Wink LK, Minshawi NF, Shaffer RC, Plawecki MH, Posey DJ, Horn PS, Adams R, Pedapati EV et al (2017) D-cycloserine enhances durability of social skills training in autism spectrum disorder. Molecular Autism 8:2. doi:10.1186/s13229-017-0116-1
18. Minshawi NF, Wink LK, Shaffer R, Plawecki MH, Posey DJ, Liu H, Hurwitz S, McDougle CJ et al (2016) A randomized, placebo-controlled trial of D-cycloserine for the enhancement of social skills training in autism spectrum disorders. Molecular Autism 7:2. doi:10.1186/s13229-015-0062-8
19. Blundell J, Blaiss CA, Etherton MR, Espinosa F, Tabuchi K, Walz C, Bolliger MF, Sudhof TC et al (2010) Neuroligin-1 deletion results in impaired spatial memory and increased repetitive behavior. The Journal of neuroscience : the official journal of the Society for Neuroscience 30(6):2115–2129. doi:10.1523/JNEUROSCI.4517-09.2010
20. Ramanathan S, Woodroffe A, Flodman PL, Mays LZ, Hanouni M, Modahl CB, Steinberg-Epstein R, Bocian ME et al (2004) A case of autism with an interstitial deletion on 4q leading to hemizygosity for genes encoding for glutamine and glycine neurotransmitter receptor sub-units (AMPA 2, GLRA3, GLRB) and neuropeptide receptors NPY1R, NPY5R. BMC Med Genet 5:10. doi:10.1186/1471-2350-5-10
21. Mead AN, Morris HV, Dixon CI, Rulten SL, Mayne LV, Zamanillo D, Stephens DN (2006) AMPA receptor GluR2, but not GluR1, subunit deletion impairs emotional response conditioning in mice. Behav Neurosci 120(2):241–248. doi:10.1037/0735-7044.120.2.241
22. Li J, Chai A, Wang L, Ma Y, Wu Z, Yu H, Mei L, Lu L et al (2015) Synaptic P-Rex1 signaling regulates hippocampal long-term depression and autism-like social behavior. Proc Natl Acad Sci U S A 112(50):E6964–E6972. doi:10.1073/pnas.1512913112
23. Nakamoto M, Nalavadi V, Epstein MP, Narayanan U, Bassell GJ, Warren ST (2007) Fragile X mental retardation protein deficiency leads to excessive mGluR5-dependent internalization of AMPA receptors. Proc Natl Acad Sci U S A 104(39):15537–15542. doi:10.1073/pnas.0707484104
24. Rouaud E, Billard JM (2003) D-cycloserine facilitates synaptic plasticity but impairs glutamatergic neurotransmission in rat hippocampal slices. Br J Pharmacol 140(6):1051–1056. doi:10.1038/sj.bjp.0705541
25. Mao SC, Lin HC, Gean PW (2008) Augmentation of fear extinction by D-cycloserine is blocked by proteasome inhibitors. Neuropsychopharmacology : official publication of the American College of Neuropsychopharmacology 33(13):3085–3095. doi:10.1038/npp.2008.30
26. Wu HF, Chen PS, Chen YJ, Lee CW, Chen IT, Lin HC (2016) Alleviation of N-methyl-D-aspartate receptor-dependent long-term depression via regulation of the glycogen synthase kinase-3beta pathway in the amygdala of a valproic acid-induced animal model of autism. Mol Neurobiol. doi:10.1007/s12035-016-0074-1
27. Kim KC, Kim P, Go HS, Choi CS, Yang SI, Cheong JH, Shin CY, Ko KH (2011) The critical period of valproate exposure to induce autistic symptoms in Sprague-Dawley rats. Toxicol Lett 201(2):137–142. doi:10.1016/j.toxlet.2010.12.018
28. Crawley JN (2004) Designing mouse behavioral tasks relevant to autistic-like behaviors. Ment Retard Dev Disabil Res Rev 10(4):248–258. doi:10.1002/mrdd.20039
29. Pellow S, Chopin P, File SE, Briley M (1985) Validation of open: closed arm entries in an elevated plus-maze as a measure of anxiety in the rat. J Neurosci Methods 14(3):149–167
30. Lacroix L, Spinelli S, Heidbreder CA, Feldon J (2000) Differential role of the medial and lateral prefrontal cortices in fear and anxiety. Behav Neurosci 114(6):1119–1130
31. Pyter LM, Pineros V, Galang JA, McClintock MK, Prendergast BJ (2009) Peripheral tumors induce depressive-like behaviors and cytokine production and alter hypothalamic-pituitary-adrenal axis regulation. Proc Natl Acad Sci U S A 106(22):9069–9074. doi:10.1073/pnas.0811949106
32. Mao SC, Chang CH, Wu CC, Orejarena MJ, Manzoni OJ, Gean PW (2013) Inhibition of spontaneous recovery of fear by mGluR5 after prolonged extinction training. PLoS One 8(3):e59580. doi:10.1371/journal.pone.0059580
33. Zhou Q, Homma KJ, Poo MM (2004) Shrinkage of dendritic spines associated with long-term depression of hippocampal synapses. Neuron 44(5):749–757. doi:10.1016/j.neuron.2004.11.011
34. Lai KO, Ip NY (2013) Structural plasticity of dendritic spines: the underlying mechanisms and its dysregulation in brain disorders. Biochim Biophys Acta 1832(12):2257–2263. doi:10.1016/j.bbadis.2013.08.012
35. Biou V, Bhattacharyya S, Malenka RC (2008) Endocytosis and recycling of AMPA receptors lacking GluR2/3. Proc Natl Acad Sci U S A 105(3):1038–1043. doi:10.1073/pnas.0711412105
36. Man HY, Lin JW, Ju WH, Ahmadian G, Liu L, Becker LE, Sheng M, Wang YT (2000) Regulation of AMPA receptor-mediated synaptic transmission by clathrin-dependent receptor internalization. Neuron 25(3):649–662
37. Wang YT, Linden DJ (2000) Expression of cerebellar long-term depression requires postsynaptic clathrin-mediated endocytosis. Neuron 25(3):635–647
38. Ahmadian G, Ju W, Liu L, Wyszynski M, Lee SH, Dunah AW, Taghibiglou C, Wang Y et al (2004) Tyrosine phosphorylation of GluR2 is required for insulin-stimulated AMPA receptor endocytosis and LTD. EMBO J 23(5):1040–1050. doi:10.1038/sj.emboj.7600126
39. Kim J, Lee S, Park K, Hong I, Song B, Son G, Park H, Kim WR et al (2007) Amygdala depotentiation and fear extinction. Proc Natl Acad Sci U S A 104(52):20955–20960. doi:10.1073/pnas.0710548105
40. Gallagher M, Chiba AA (1996) The amygdala and emotion. Curr Opin Neurobiol 6(2):221–227
41. Baron-Cohen S, Ring HA, Bullmore ET, Wheelwright S, Ashwin C, Williams SC (2000) The amygdala theory of autism. Neurosci Biobehav Rev 24(3):355–364
42. Baxter MG, Croxson PL (2012) Facing the role of the amygdala in emotional information processing. Proc Natl Acad Sci U S A 109(52):21180–21181. doi:10.1073/pnas.1219167110
43. Huang TN, Chuang HC, Chou WH, Chen CY, Wang HF, Chou SJ, Hsueh YP (2014) Tbr1 haploinsufficiency impairs amygdalar axonal projections and results in cognitive abnormality. Nat Neurosci 17(2):240–247. doi:10.1038/nn.3626
44. Lin HC, Gean PW, Wang CC, Chan YH, Chen PS (2013) The amygdala excitatory/inhibitory balance in a valproate-induced rat autism model. PLoS One 8(1):e55248. doi:10.1371/journal.pone.0055248
45. Chen YW, Lin HC, Ng MC, Hsiao YH, Wang CC, Gean PW, Chen PS (2014) Activation of mGluR2/3 underlies the effects of N-acetylcystein on amygdala-associated autism-like phenotypes in a

valproate-induced rat model of autism. Front Behav Neurosci 8: 219. doi:10.3389/fnbeh.2014.00219
46. Markram K, Rinaldi T, La Mendola D, Sandi C, Markram H (2008) Abnormal fear conditioning and amygdala processing in an animal model of autism. Neuropsychopharmacol: Off Publ Am College Neuropsychopharmacology 33(4):901–912. doi:10.1038/sj.npp.1301453
47. O'Roak BJ, Vives L, Fu W, Egertson JD, Stanaway IB, Phelps IG, Carvill G, Kumar A et al (2012) Multiplex targeted sequencing identifies recurrently mutated genes in autism spectrum disorders. Science 338(6114):1619–1622. doi:10.1126/science.1227764
48. Kenny EM, Cormican P, Furlong S, Heron E, Kenny G, Fahey C, Kelleher E, Ennis S et al (2014) Excess of rare novel loss-of-function variants in synaptic genes in schizophrenia and autism spectrum disorders. Mol Psychiatry 19(8):872–879. doi:10.1038/mp.2013.127
49. Tarabeux J, Kebir O, Gauthier J, Hamdan FF, Xiong L, Piton A, Spiegelman D, Henrion E et al (2011) Rare mutations in N-methyl-D-aspartate glutamate receptors in autism spectrum disorders and schizophrenia. Transl Psychiatry 1:e55. doi:10.1038/tp.2011.52
50. Yoo HJ, Cho IH, Park M, Yang SY, Kim SA (2012) Family based association of GRIN2A and GRIN2B with Korean autism spectrum disorders. Neurosci Lett 512(2):89–93. doi:10.1016/j.neulet.2012.01.061
51. Lee EJ, Choi SY, Kim E (2015) NMDA receptor dysfunction in autism spectrum disorders. Curr Opin Pharmacol 20:8–13. doi:10.1016/j.coph.2014.10.007
52. Lee E, Lee J, Kim E (2016) Excitation/inhibition imbalance in animal models of autism spectrum disorders. Biol Psychiatry. doi:10.1016/j.biopsych.2016.05.011
53. Pilorge M, Fassier C, Le Corronc H, Potey A, Bai J, De Gois S, Delaby E, Assouline B et al (2016) Genetic and functional analyses demonstrate a role for abnormal glycinergic signaling in autism. Mol Psychiatry 21(7):936–945. doi:10.1038/mp.2015.139
54. Rinaldi T, Kulangara K, Antoniello K, Markram H (2007) Elevated NMDA receptor levels and enhanced postsynaptic long-term potentiation induced by prenatal exposure to valproic acid. Proc Natl Acad Sci U S A 104(33):13501–13506. doi:10.1073/pnas.0704391104
55. Kang J, Kim E (2015) Suppression of NMDA receptor function in mice prenatally exposed to valproic acid improves social deficits and repetitive behaviors. Front Mol Neurosci 8:17. doi:10.3389/fnmol.2015.00017
56. Dhawan J, Benveniste H, Luo Z, Nawrocky M, Smith SD, Biegon A (2011) A new look at glutamate and ischemia: NMDA agonist improves long-term functional outcome in a rat model of stroke. Future Neurol 6(6):823–834. doi:10.2217/fnl.11.55
57. Adeleye A, Shohami E, Nachman D, Alexandrovich A, Trembovler V, Yaka R, Shoshan Y, Dhawan J et al (2010) D-cycloserine improves functional outcome after traumatic brain injury with wide therapeutic window. Eur J Pharmacol 629(1–3):25–30. doi:10.1016/j.ejphar.2009.11.066
58. Malenka RC, Nicoll RA (1993) NMDA-receptor-dependent synaptic plasticity: multiple forms and mechanisms. Trends Neurosci 16(12):521–527
59. Hunt DL, Castillo PE (2012) Synaptic plasticity of NMDA receptors: mechanisms and functional implications. Curr Opin Neurobiol 22(3):496–508. doi:10.1016/j.conb.2012.01.007
60. Beattie EC, Carroll RC, Yu X, Morishita W, Yasuda H, von Zastrow M, Malenka RC (2000) Regulation of AMPA receptor endocytosis by a signaling mechanism shared with LTD. Nat Neurosci 3(12): 1291–1300. doi:10.1038/81823
61. Lu W, Man H, Ju W, Trimble WS, MacDonald JF, Wang YT (2001) Activation of synaptic NMDA receptors induces membrane insertion of new AMPA receptors and LTP in cultured hippocampal neurons. Neuron 29(1):243–254
62. Chanda S, Aoto J, Lee SJ, Wernig M, Sudhof TC (2016) Pathogenic mechanism of an autism-associated neuroligin mutation involves altered AMPA-receptor trafficking. Mol Psychiatry 21(2):169–177. doi:10.1038/mp.2015.20
63. Li W, Xu X, Pozzo-Miller L (2016) Excitatory synapses are stronger in the hippocampus of Rett syndrome mice due to altered synaptic trafficking of AMPA-type glutamate receptors. Proc Natl Acad Sci U S A 113(11):E1575–E1584. doi:10.1073/pnas.1517244113
64. Mejias R, Adamczyk A, Anggono V, Niranjan T, Thomas GM, Sharma K, Skinner C, Schwartz CE et al (2011) Gain-of-function glutamate receptor interacting protein 1 variants alter GluA2 recycling and surface distribution in patients with autism. Proc Natl Acad Sci U S A 108(12):4920–4925. doi:10.1073/pnas.1102233108
65. Han M, Mejias R, Chiu SL, Rose R, Adamczyk A, Huganir R, Wang T (2017) Mice lacking GRIP1/2 show increased social interactions and enhanced phosphorylation at GluA2-S880. Behav Brain Res 321:176–184. doi:10.1016/j.bbr.2016.12.042
66. Tan HL, Queenan BN, Huganir RL (2015) GRIP1 is required for homeostatic regulation of AMPAR trafficking. Proc Natl Acad Sci U S A 112(32):10026–10031. doi:10.1073/pnas.1512786112
67. Duan TT, Tan JW, Yuan Q, Cao J, Zhou QX, Xu L (2013) Acute ketamine induces hippocampal synaptic depression and spatial memory impairment through dopamine D1/D5 receptors. Psychopharmacology 228(3):451–461. doi:10.1007/s00213-013-3048-2
68. Penzes P, Cahill ME, Jones KA, VanLeeuwen JE, Woolfrey KM (2011) Dendritic spine pathology in neuropsychiatric disorders. Nat Neurosci 14(3):285–293. doi:10.1038/nn.2741
69. Ultanir SK, Kim JE, Hall BJ, Deerinck T, Ellisman M, Ghosh A (2007) Regulation of spine morphology and spine density by NMDA receptor signaling in vivo. Proc Natl Acad Sci U S A 104(49):19553–19558. doi:10.1073/pnas.0704031104
70. Alvarez VA, Ridenour DA, Sabatini BL (2007) Distinct structural and ionotropic roles of NMDA receptors in controlling spine and synapse stability. J Neurosci 27(28):7365–7376. doi:10.1523/JNEUROSCI.0956-07.2007
71. Chen BS, Thomas EV, Sanz-Clemente A, Roche KW (2011) NMDA receptor-dependent regulation of dendritic spine morphology by SAP102 splice variants. J Neurosci 31(1):89–96. doi:10.1523/JNEUROSCI.1034-10.2011
72. Gupta SC, Yadav R, Pavuluri R, Morley BJ, Stairs DJ, Dravid SM (2015) Essential role of GluD1 in dendritic spine development and GluN2B to GluN2A NMDAR subunit switch in the cortex and hippocampus reveals ability of GluN2B inhibition in correcting hyperconnectivity. Neuropharmacology 93:274–284. doi:10.1016/j.neuropharm.2015.02.013
73. Lamprecht R, Farb CR, Rodrigues SM, LeDoux JE (2006) Fear conditioning drives profilin into amygdala dendritic spines. Nat Neurosci 9(4):481–483. doi:10.1038/nn1672
74. Radley JJ, Johnson LR, Janssen WG, Martino J, Lamprecht R, Hof PR, LeDoux JE, Morrison JH (2006) Associative Pavlovian conditioning leads to an increase in spinophilin-immunoreactive dendritic spines in the lateral amygdala. Eur J Neurosci 24(3):876–884. doi:10.1111/j.1460-9568.2006.04962.x
75. Calabrese B, Saffin JM, Halpain S (2014) Activity-dependent dendritic spine shrinkage and growth involve downregulation of cofilin via distinct mechanisms. PLoS One 9(4):e94787. doi:10.1371/journal.pone.0094787
76. Leuner B, Shors TJ (2004) New spines, new memories. Mol Neurobiol 29(2):117–130. doi:10.1385/MN:29:2:117